Published in final edited form as:
*Structure*. 2007 June ; 15(6): 707–714.

# Structure of synaptophysin: A hexameric MARVEL domain channel protein

**Christopher P. Arthur**[1] and **Michael H. B. Stowell**[1]
***1*** *MCD Biology, University of Colorado, Boulder, CO 80309*

## Abstract

Synaptophysin 1 is an archetypal member of the MARVEL domain family of integral membrane proteins and one of the first synaptic vesicle proteins to be identified and cloned (Rehm et al., 1986;Sanchez-Pulido et al., 2002). Most all MARVEL domain proteins are involved in membrane apposition and vesicle trafficking events but their precise role in these processes is unclear. We have purified mammalian Syp1 and determined its three-dimensional structure using electron microscopy and single-particle 3-D reconstruction. The hexameric structure resembles an open basket with a large pore and tenuous interactions within the cytosolic domain. The structure suggests a model for synaptophysin's role in fusion and recycling that is regulated by known interactions with the SNARE machinery. This is the first three dimensional structure of a MARVEL domain protein and provides a structural foundation for understanding the role of these important proteins in a variety of biological processes.

## Introduction

Neurotransmitter release is a highly regulated process comprised of a series of steps that include: the targeting of synaptic vesicles (SV) to pre-synaptic active zones, the anchoring of SVs to the plasma membrane, the fusion of the SV membrane with the plasma membrane upon stimulation, and the recycling of the SV membrane and machinery back into a functional SV (Sudhof, 2000). The process of exocytosis during neurotransmitter release has been studied extensively and several conserved families of proteins have been shown to reside within the SVs membrane (De Camilli and Jahn, 1990). One such protein is Syp1, which comprises ~8% of total SV proteins (Rehm et al., 1986). Synaptophysin 1 (Syp1) is a member of the physin family which consists of synaptophysin, synaptoporin, pantophysin (sypl1), mitsugumin (sypl2), and synaptogyrin (Janz et al., 1999;Leube, 1994) (Figure 1A). While a definitive role of physins and synaptogyrins in the vesicle cycle is lacking, evidence indicates that they are a component of the vesicle trafficking machinery (Janz et al., 1999). Physiologically it has been observed that Syp1 undergoes a major cellular redistribution in schizophrenia (Eastwood and Harrison, 2001), although how this relates to the disease is unclear.

Syp1 is a 38 kDa integral membrane protein which is a member of the MARVEL (MAL and Related proteins for VEsicle trafficking and membrane Link) family of integral membrane proteins associated with membrane juxtapositions (Sanchez-Pulido et al., 2002). Based on amino acid sequences the predicted secondary structure of mammalian Syp1 consists of four

Correspondence and requests for materials should be addressed to M.H.B.S. (stowellm@colorado.edu).

The authors declare no competing financial interests.

transmembrane α-helices, two intravesicular loops, and cytoplasmic N- and C-termini. The C-terminus contains a $Ca^{2+}$ binding motif and ten pentapeptide repeats, nine of which contain tyrosine residues which are phosphorylated by Src *in vitro* (Evans and Cousin, 2005;Rehm et al., 1986).

Although Syp1 is the most abundant protein on SVs, surprisingly little is known about its involvement in the SV cycle or its physiological role in neurotransmitter release. Several experiments have been performed in an attempt to explain Syp1's function. Early studies proposed that synaptophysin was a negative regulator of vesicle fusion as a consequence of its interaction with the v-SNARE synaptobrevin (Becher et al., 1999). Studies in *Xenopus* oocyte reconstitution systems suggested Syp1 has a role in neurotransmitter release but precisely what role was unclear (Valtorta et al., 2004). In contrast, studies of Syp1 knockout mice showed no pronounced phenotype and presumably Syp1 had no distinct function in the vesicle cycle (Eshkind and Leube, 1995;Janz et al., 1999). While at least three other isoforms of Syp1 have been identified that could developmentally compensate for loss of SypI activity it appears that at least transcriptionally this is not the case (Bai et al., 2006). Intriguingly a double knockout of Syp1 and synaptogyrin shows a pronounced reduction in synaptic plasticity even though evoked neurotransmitter release was still apparently normal. Electron microscopy examination of the morphology of retinal photoreceptors in the Syp1/synaptogyrin knockout mice revealed a defect in SV endocytosis (Spiwoks-Becker et al., 2001;Valtorta et al., 2004) and an increase in the number of clathrin-coated vesicles suggested a selective inhibition of clathrin-independent endocytosis. Further evidence for Syp1's involvement in SV endocytosis is that the major Syp1 binding partner on SVs, synaptobrevin (Syb), has been implicated in a form of endocytosis that rapidly recycles SVs following exocytosis (Dittman and Kaplan, 2006). Regardless of the precise function of Syp1, it must participate in the vesicle cycle at some stage and its identification as a member of the MARVEL family of membrane proteins involved in membrane juxtapositions further suggests it may have a role in fusion and recycling. While physiologically Syp1 does not have an essential role it is most likely important for fine tuning of neurotransmitter release which effects memory and learning phenomenon such as LTP. This higher order function appears to be related to the phosphorylation of synaptophysin which occurs following LTP stimulation protocols (Evans and Cousin, 2005).

Structurally, Syp1 has been observed to form a multimer which, when reconstituted into a planar lipid bilayer, forms voltage-dependent channels with a conductance similar to gap junctions and mechanosensitive channel (Bass et al., 2002;Gincel and Shoshan-Barmatz, 2002;Perozo et al., 2002;Rehm et al., 1986;Unger et al., 1999). While Syp1 and the gap junction protein connexin share very little sequence homology, they do share similar membrane topologies and strong similarity within their third transmembrane domain (Leube, 1995) (Figure 1B). Interestingly, this third transmembrane domain of connexin lines the gap junction pore and, by analogy, perhaps the fusion pore of Syp1. While it has been proposed that Syp1 may be the main component of a potential fusion pore complex which forms during transient fusion events involving SVs, no structural work has been done to verify that Syp1 forms a channel-like structure that would be compatible with such an hypothesis (Pennuto et al., 2002;Valtorta et al., 2004). Here we report the first three dimensional structural analysis of the Syp1 complex at 20 Å resolution using negative stain electron microscopy and computational image processing. The structure reveals that Syp1 forms a hexameric basket-like complex with a closed conformation on the cytosolic side of the membrane and an extended open conformation on the vesicle lumen side and large pore within the membrane and suggests how Syp1 may be involved in the vesicle cycle.

## Results

The Syp1 structure resembles multimeric mechanosensitive channels and gap junction hemi-channels and is consistent with the hypothetical role of Syp1 as a neurotransmitter channel that disassociates during vesicle fusion. The 3D map generated for Syp1 (Figure 2C) has dimensions of ~70 Å X ~70 Å overall height and diameter, with an enclosed volume of ~226,000 $Å^3$. This is comparable to the calculated volume for a 240 kDa Syp1 hexamer (~197,000 $Å^3$) (Fischer et al., 2004). The structure shows a basket-like formation with six individual spokes of density radiating outward and upwards from a central hub. The structure also shows an apparent handedness which is seen in many biological structures (Bass et al., 2002;Perozo et al., 2002). During the reconstruction a six-fold symmetry was imposed to generate the final 3-D map. Results of cross-linking analysis along with gel filtration chromatography of purified Syp1 complex lead us to believe that Syp1 indeed exists as a hexamer *in vivo* (Figure 3A). In order to verify that our final reconstruction was accurate we performed subsequent reconstructions using the same data but imposing either five-fold or seven-fold symmetry (Figure 3D). Neither of these reconstructions generated a coherent model.

Based on the predicted membrane topology of Syp1 (Figure 1A) and its similarity to the gap junction complex, we were able to dock a previously determined model (Fleishman et al., 2004) of the transmembrane segment of the gap junction into our density map (Figure 2D & E). The docking allows us to delineate the area of the plasma membrane and assign an orientation of Syp1. Based upon the amino acid sequence and expected volume occupied by the intra-transmembrane loops, we have assigned the open end of the structure within the vesicle lumen, and the closed end containing the N- and C-termini on the cytosolic side of the vesicle membrane (Figure 2C–E). The third transmembrane domain of connexin has been shown to line the gap junction pore and by analogy we docked the transmembrane domain structure in a similar orientation allowing for the possibility that the third transmembrane domain of Syp1 may line the interior of the Syp1 fusion pore complex.

## Discussion

The intermediate resolution model which we have generated bares a striking resemblance to other known channel structures, in particular the gap junction and mechanosensitive channels, both of which have similar conductances to the Syp1 channel (Figure 4). The overall dimensions of these channels are quite similar as well. Our Syp1 structure has an outer diameter of ~70 Å, with an inner diameter of ~30 Å; these are the similar dimensions of connexin (Unger et al., 1999) and very close to the dimensions of MscS (80 Å diameter, 25 Å pore) (Bass et al., 2002). The apparently loose intersubunit intramembrane interactions suggest how Syp1 may interact with Syb and function as a mechanosensitive channel where the SNARE complex formation drives disassembly of the Syp1/Syb multimer leading to channel opening and neurotransmitter release (Figure 5). Recent work has shown that the fusion pore involved in neurotransmitter release has a conductance of ~.375 nS and that the potential pore diameter based on this conductance should be in the order of >2.3 nm (He et al., 2006). These numbers correlate very well with the three dimensional structure we have generated.

There are two observed mechanisms of vesicle fusion and recycling at the pre-synaptic active zone: full fusion and transient fusion (also known as Kiss-and-Run) (Sudhof, 2000). In the full fusion model, SVs are docked at the pre-synaptic membrane by a potential interaction of Syb on the vesicle surface and syntaxin (Syx) on the plasma membrane (Figure 5 step 1). These proteins are thought to potentially be held together by SNAP25 and complexin (Tang et al., 2006). Upon depolarization of the neuronal membrane and influx of $Ca^{2+}$, Synaptotagmin I (SytI) binds to the SNARE complex and its $Ca^{2+}$ binding C2 domains form a tight electrostatic interaction with the plasma membrane. A subsequent coiled coil is formed by the SNARE

complex (Syx, Syb, and SNAP-25) thus drawing in the SV to fully fuse with the plasma membrane (Figure 5 step 2 & 3) (Hui et al., 2006). During transient fusion the SV is also drawn in close to the plasma membrane upon depolarization and $Ca^{2+}$ influx. However, the SV never fully fuses with the plasma membrane, only a transient fusion pore is formed for neurotransmitter release and the intact SV is eventually released back from the membrane and re-primed for another fusion event (Figure 5 step 2* & 3*). Currently, the molecular mechanism of transient fusion is not known. Multiple proteins have been proposed as contributors and/or regulators of transient fusion, including Syp1, however, the roles of these proteins has not been confirmed (Fernandez-Alfonso and Ryan, 2004;Harata et al., 2006;Wang et al., 2006;Wang et al., 2003).

Based on our structure and published biochemical data on Syp1 and other SV proteins including SytI, Syb, Syx, and synaptotagmin IV (SytIV), we have derived the following model for a possible role of Syp1 in pore formation during full and transient SV fusion. Syb is known to bind to multiple SV proteins exclusive of SNARE complex formation including Syp1 and SytIV [17,26]. SytIV has been implicated in transient fusion (Wang et al., 2003), although to what extent is unclear. Increased expression of SytIV leads to an increase in kiss-and-run events, and removal of SytIV leads to a disability in memory function associated with neurotransmitter release (Ferguson et al., 2000) and a loss of SVs (Dean C., Arthur C., Bhalla A., Liu H., Chang P., Stowell M., Jackson M. B., & Chapman E. R. Activity dependent modulation of synaptic vesicle composition regulates synaptic plasticity. submitted) SytIV has also been shown to compete with SytI for SNARE binding (Machado et al., 2004). We propose that the interaction of SytIV with the Syb/Syp1 complex can regulate the choice between kiss-and-run and full fusion. In our model, Syb and Syp1 are bound in a multimeric complex with SytIV prior to the SV being docked at the active zone (Figure 5 step 1). Upon membrane depolarization, SytIV binds weakly with the pre-synaptic membrane, Syb is inhibited by Syp1 from entering the coiled-coil SNARE complex and the Syb/Syp1 complex remains stable forming a fusion pore potentially with Syx, another complex on the plasma membrane which has been shown to be active in neurotransmitter release (Figure 5 step 2*) (Han et al., 2004). The SytIV/plasma membrane interaction is not as strong as the SytI/plasma membrane interaction and no full SNARE complex is formed. The Syx/Syp1 fusion pore dissociates, potentially upon interaction with dynamin and the SV does not go through full fusion (Figure 5 step 3*). In this model the exclusion of SytI from the binding machinery inhibits the vesicle from undergoing complete exocytosis. In the full-fusion model, the strong interaction of SytI with the plasma membrane allows the formation of the complete SNARE complex and this strong interaction acts to dissociate Syb from the Syp1 complex thus allowing the Syp1 complex to destabilize and full vesicle fusion to occur (Figure 5 step 3).

The four transmembrane-helix architecture which makes up the MARVEL domain in Syp1 is seen in a number of other protein families including the myelin and lymphocyte protein (MAL), synaptogyrin and occluding (Sanchez-Pulido et al., 2002). The involvement of all of these MARVEL domain proteins with membrane contact and interaction is strong evidence for Syp1's role in vesicle membrane interaction at the plasma membrane. The structure of Syp1 described here provides the first three dimensional data for a MARVEL domain protein and suggests how Syp1 may form a fusion pore complex which regulates synaptic vesicle exocytosis. While further studies are required to fully elucidate the function and mechanism of SypI, as well as other MARVEL domain proteins, our results provide a structural foundation for understanding these important and ubiquitous proteins.

## Materials and Methods

### SV preparation

SVs were prepared from frozen calf brain as described previously (Huttner et al., 1983). Briefly, 20g of frozen tissue was homogenized in a buffer solution (4 mM HEPES (pH 7.3), 0.32 M sucrose). Homogenate was centrifuged at 800*g* for 15 minutes (4° C). Supernatant was removed and centrifuged at 9,200*g* for 20 minutes (4° C). Pellet was resuspended in an equivolume of homogenization buffer and centrifuged at 10,200*g* for 20 minutes (4° C). Pellet was resuspended in 40 ml of homogenization buffer. Resuspended pellet was diluted 1:10 with ice cold $dH_2O$. This suspension was subjected to three up-and-down strokes in a glass homogenizer. The resulting lysate was poured rapidly into 9 ml of 1 M HEPES (pH7.3), and the suspension was incubated on ice for 30 minutes. The suspension was then centrifuged at 25,000*g* for 20 minutes (4° C), the supernatant was removed and centrifuged at 165,000*g* for 2 hours (4° C). Pellet was resuspended in 10 ml of 40 mM sucrose and the suspension was layered on top of a continuous sucrose gradient. Sucrose gradient was centrifuged at 65,000*g* for 5 hours (4° C). At the end of centrifugation the gradient revealed a broad band of high turbidity at the 200–400 mM sucrose region, which, from previous experiments (Fukuda, 2002) is known to be enriched in SVs. This band was collected and further processed for SypI purification.

### SypI purification

Purified SVs were incubated for 30 minutes at 0° C (at 5 mg/ml) in a solution containing 5 mM $NaH_2PO_4$ (pH6.8), and 0.2% Triton X-100 (w/v). The Triton X-100 extract was centrifuged at 45,000*g* for 30 minutes (4° C). Supernatant was applied to a dry hydroxyapatite/celite column (2:1 w/w) (0.1 g/mg protein) and eluted with solubilization buffer. The resin bound proteins were eluted and found to contain no SypI. The SypI containing flow through was applied to a POROS H10 anion-exchange column and eluted using a NaCl gradient from 0–1 M (20 mM $NaH_2PO_4$ (pH6.8), 0.2% Brij-35, 40 mM sucrose). 1 ml fractions were collected and analyzed using SDS-PAGE. Fractions containing SypI were combined and flowed over Hi-Prep Sephacryl S-300 size-exclusion column. Protein was eluted using 20 mM $NaH_2PO_4$ (pH6.8), 0.2% Brij-35, 40 mM sucrose. Fractions were analyzed using SDS-PAGE and western blotting techniques. Blots were probed with monoclonal SypI antibodies. Fractions of purified SypI were combined (Figure 3B).

### Electron microscopy

Purified SypI (50μg/ml) was applied to a freshly carbon coated, glow-discharged EM grid and stained using 2% ammonium molybdate (Hoenger and Aebi, 1996). Images were recorded under low-dose conditions at a magnification of 50,000 and at a defocus range of 1–3μm using a Tecnai F20 microscope at 200 keV equipped with a Gatan 2K X 2K CCD camera. The pixel size was 0.45 nm.

### Image processing

Individual SypI particles were selected and boxed, and image analysis was performed using the EMAN image processing package (Ludtke et al., 1999). Briefly, an initial model was generated using the raw boxed particles and an imposed sixfold symmetry (based on size exclusion chromatography data which tells us that SypI is a hexamer (Figure 3A)). From this initial model angular projections were generated and particles were again classified based on these projections. From these classifications a new model was generated and the process was repeated. The final model was a result of 8 rounds of refinement and contained ~1200 particles. The resolution of the final model was calculated to be ~30 Å based on FSC using a standard cutoff of 0.5 (Figure 3C).

**Acknowledgements**

We thank our colleagues at the University of Colorado for their support. We thank E. R. Chapman, A. Hoenger, R. A. Milligan, A. B. Ward, and M. W. Klymkowsky for comments on the manuscript. C.P.A. was supported by the NIH/CU Molecular Biophysics Training Program (NIH **T32 GM065103**). This work was supported in part by the Human Frontier Science Program and the Beckman Foundation (M.H.B.S.).

## References

Bai L, Spiwoks-Becker I, Leube RE. Transcriptome comparison of murine wild-type and synaptophysin-deficient retina reveals complete identity. Brain Res 2006;1081:53–58. [PubMed: 16519878]

Bass RB, Strop P, Barclay M, Rees DC. Crystal structure of Escherichia coli MscS, a voltage-modulated and mechanosensitive channel. Science 2002;298:1582–1587. [PubMed: 12446901]

Becher A, Drenckhahn A, Pahner I, Margittai M, Jahn R, Ahnert-Hilger G. The synaptophysin-synaptobrevin complex: a hallmark of synaptic vesicle maturation. J Neurosci 1999;19:1922–1931. [PubMed: 10066245]

De Camilli P, Jahn R. Pathways to regulated exocytosis in neurons. Annu Rev Physiol 1990;52:625–645. [PubMed: 2184771]

Dittman JS, Kaplan JM. Factors regulating the abundance and localization of synaptobrevin in the plasma membrane. Proc Natl Acad Sci U S A 2006;103:11399–11404. [PubMed: 16844789]

Eastwood SL, Harrison PJ. Synaptic pathology in the anterior cingulate cortex in schizophrenia and mood disorders. A review and a Western blot study of synaptophysin, GAP-43 and the complexins. Brain Res Bull 2001;55:569–578. [PubMed: 11576753]

Eshkind LG, Leube RE. Mice lacking synaptophysin reproduce and form typical synaptic vesicles. Cell Tissue Res 1995;282:423–433. [PubMed: 8581936]

Evans GJ, Cousin MA. Tyrosine phosphorylation of synaptophysin in synaptic vesicle recycling. Biochem Soc Trans 2005;33:1350–1353. [PubMed: 16246116]

Ferguson GD, Anagnostaras SG, Silva AJ, Herschman HR. Deficits in memory and motor performance in synaptotagmin IV mutant mice. Proc Natl Acad Sci U S A 2000;97:5598–5603. [PubMed: 10792055]

Fernandez-Alfonso T, Ryan TA. The kinetics of synaptic vesicle pool depletion at CNS synaptic terminals. Neuron 2004;41:943–953. [PubMed: 15046726]

Fischer H, Polikarpov I, Craievich AF. Average protein density is a molecular-weight-dependent function. Protein Sci 2004;13:2825–2828. [PubMed: 15388866]

Fleishman SJ, Unger VM, Yeager M, Ben-Tal N. A Calpha model for the transmembrane alpha helices of gap junction intercellular channels. Mol Cell 2004;15:879–888. [PubMed: 15383278]

Fukuda M. Vesicle-associated membrane protein-2/synaptobrevin binding to synaptotagmin I promotes O-glycosylation of synaptotagmin I. J Biol Chem 2002;277:30351–30358. [PubMed: 12048209]

Gincel D, Shoshan-Barmatz V. The synaptic vesicle protein synaptophysin: purification and characterization of its channel activity. Biophys J 2002;83:3223–3229. [PubMed: 12496091]

Han X, Wang CT, Bai J, Chapman ER, Jackson MB. Transmembrane segments of syntaxin line the fusion pore of Ca2+-triggered exocytosis. Science 2004;304:289–292. [PubMed: 15016962]

Harata NC, Aravanis AM, Tsien RW. Kiss-and-run and full-collapse fusion as modes of exo-endocytosis in neurosecretion. J Neurochem 2006;97:1546–1570. [PubMed: 16805768]

He L, Wu XS, Mohan R, Wu LG. Two modes of fusion pore opening revealed by cell-attached recordings at a synapse. Nature 2006;444:102–105. [PubMed: 17065984]

Hoenger A, Aebi U. 3-D Reconstructions from Ice-Embedded and Negatively Stained Biomacromolecular Assemblies: A Critical Comparison. Journal of Structural Biology 1996;117:99–116.

Hui E, Bai J, Chapman ER. Ca2+-triggered simultaneous membrane penetration of the tandem C2-domains of synaptotagmin I. Biophys J 2006;91:1767–1777. [PubMed: 16782782]

Huttner WB, Schiebler W, Greengard P, De Camilli P. Synapsin I (protein I), a nerve terminal-specific phosphoprotein. III. Its association with synaptic vesicles studied in a highly purified synaptic vesicle preparation. J Cell Biol 1983;96:1374–1388. [PubMed: 6404912]

Janz R, Sudhof TC, Hammer RE, Unni V, Siegelbaum SA, Bolshakov VY. Essential roles in synaptic plasticity for synaptogyrin I and synaptophysin I. Neuron 1999;24:687–700. [PubMed: 10595519]

Leube RE. Expression of the synaptophysin gene family is not restricted to neuronal and neuroendocrine differentiation in rat and human. Differentiation 1994;56:163–171. [PubMed: 8034131]

Leube RE. The topogenic fate of the polytopic transmembrane proteins, synaptophysin and connexin, is determined by their membrane-spanning domains. J Cell Sci 1995;108(Pt 3):883–894. [PubMed: 7622617]

Ludtke SJ, Baldwin PR, Chiu W. EMAN: semiautomated software for high-resolution single-particle reconstructions. J Struct Biol 1999;128:82–97. [PubMed: 10600563]

Machado HB, Liu W, Vician LJ, Herschman HR. Synaptotagmin IV overexpression inhibits depolarization-induced exocytosis in PC12 cells. J Neurosci Res 2004;76:334–341. [PubMed: 15079862]

Pennuto M, Dunlap D, Contestabile A, Benfenati F, Valtorta F. Fluorescence resonance energy transfer detection of synaptophysin I and vesicle-associated membrane protein 2 interactions during exocytosis from single live synapses. Mol Biol Cell 2002;13:2706–2717. [PubMed: 12181340]

Perozo E, Cortes DM, Sompornpisut P, Kloda A, Martinac B. Open channel structure of MscL and the gating mechanism of mechanosensitive channels. Nature 2002;418:942–948. [PubMed: 12198539]

Rehm H, Wiedenmann B, Betz H. Molecular characterization of synaptophysin, a major calcium-binding protein of the synaptic vesicle membrane. Embo J 1986;5:535–541. [PubMed: 3086086]

Sanchez-Pulido L, Martin-Belmonte F, Valencia A, Alonso MA. MARVEL: a conserved domain involved in membrane apposition events. Trends Biochem Sci 2002;27:599–601. [PubMed: 12468223]

Spiwoks-Becker I, Vollrath L, Seeliger MW, Jaissle G, Eshkind LG, Leube RE. Synaptic vesicle alterations in rod photoreceptors of synaptophysin-deficient mice. Neuroscience 2001;107:127–142. [PubMed: 11744253]

Sudhof TC. The synaptic vesicle cycle revisited. Neuron 2000;28:317–320. [PubMed: 11144340]

Tang J, Maximov A, Shin OH, Dai H, Rizo J, Sudhof TC. A complexin/synaptotagmin 1 switch controls fast synaptic vesicle exocytosis. Cell 2006;126:1175–1187. [PubMed: 16990140]

Unger VM, Kumar NM, Gilula NB, Yeager M. Three-dimensional structure of a recombinant gap junction membrane channel. Science 1999;283:1176–1180. [PubMed: 10024245]

Valtorta F, Pennuto M, Bonanomi D, Benfenati F. Synaptophysin: leading actor or walk-on role in synaptic vesicle exocytosis? Bioessays 2004;26:445–453. [PubMed: 15057942]

Wang CT, Bai J, Chang PY, Chapman ER, Jackson MB. Synaptotagmin-Ca2+ triggers two sequential steps in regulated exocytosis in rat PC12 cells: fusion pore opening and fusion pore dilation. J Physiol 2006;570:295–307. [PubMed: 16293646]

Wang CT, Lu JC, Bai J, Chang PY, Martin TF, Chapman ER, Jackson MB. Different domains of synaptotagmin control the choice between kiss-and-run and full fusion. Nature 2003;424:943–947. [PubMed: 12931189]

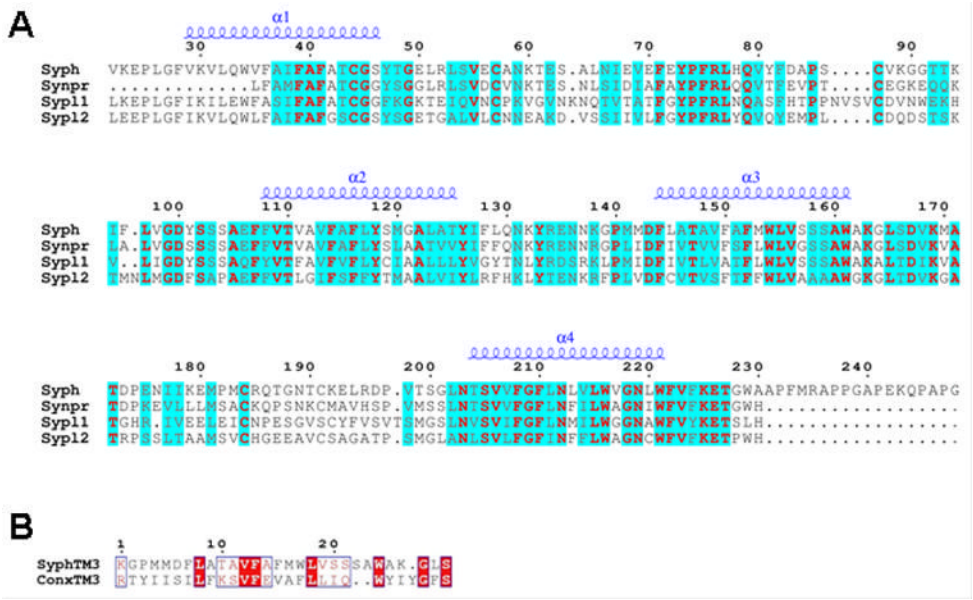


**Figure 1. Comparison of transmembrane domains of synaptophysin family proteins and sequence alignment of Synaptophysin and Connexin**

(A) Sequences are taken from the following: mouse synaptophysin I (Syph), mouse synaptoporin (Synpr), mouse synaptophysin-like protein 1 (Sypl1) and mouse synaptophysin-like protein 2 (Sypl2). These proteins are known to reside on synaptic vesicles and may account for the lack of phenotype seen when individual members of this family are removed. (B) Sequence alignment of the third transmembrane segment of Syp1 (SyphTM3) and the third transmembrane segment of connexin α 1 (ConxTM3).

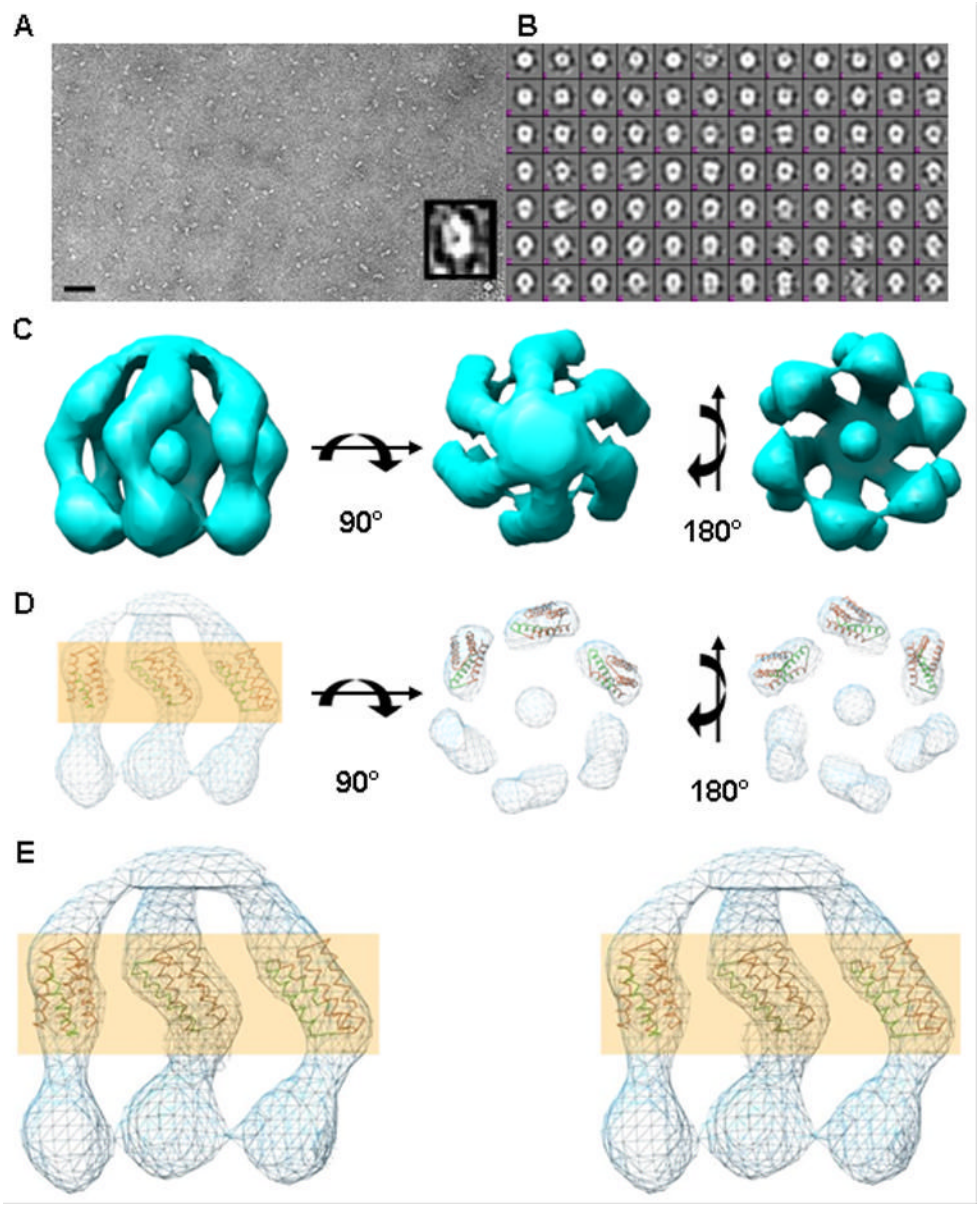


**Figure 2. Single particle electron microscopy of negatively stained synaptophysin I**

(A) Low dose image of synaptophysin I complexes negatively stained with 2% ammonium molybdate on continuous carbon substrate. (Inset) magnified image of single synaptophysin I complex (scale bar = 100 nm). (B) Gallery of representative class averages displaying various views of the synaptophysin I complex. (C) Three views of the surface rendered density map of the synaptophysin I complex rendered at 20 Å resolution. The structure shows an overall diameter of 70 Å with an inner diameter of 30 Å. Density is contoured to 2.0 σ. (D) Mesh view of (C) with connexin docked into the density map. Highlighted area represents the lipid bilayer. (E) Stereo mesh view of (D) truncated to show the inner wall of the complex. The atomic model of connexin is docked into the density map with the third transmembrane domain represented in green. Highlighted area represents the lipid bilayer.

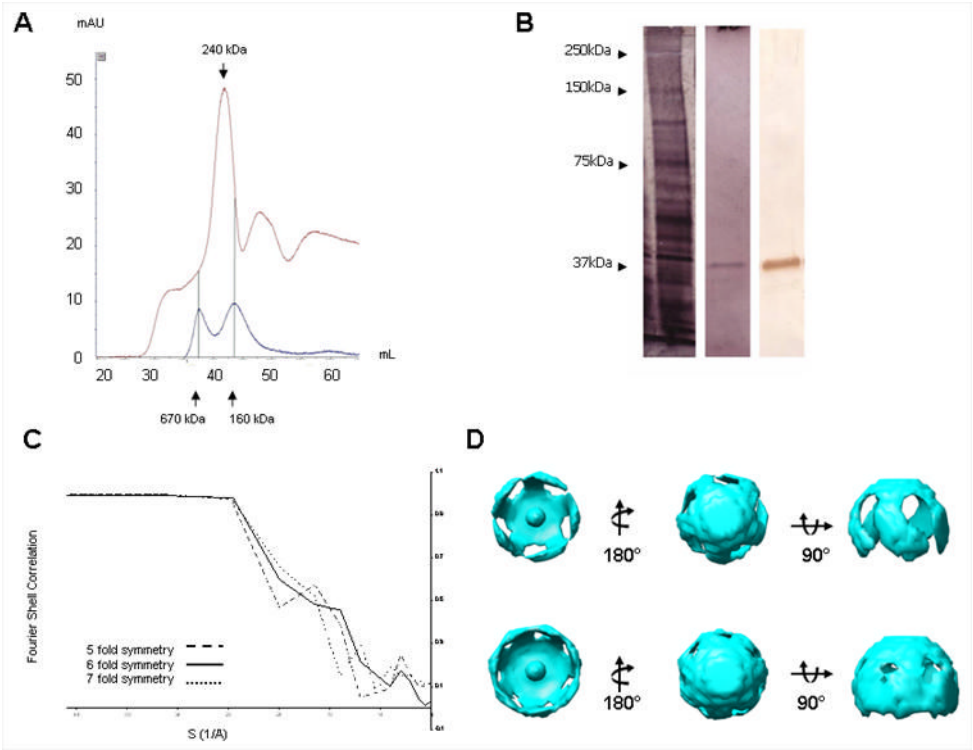


**Figure 3. Chromatogram from gel filtration purification of synaptophysin I complex. Resolution analysis of synaptophysin I three-dimensional reconstruction and models of 5-fold and 7-fold imposed symmetry. Resolution analysis of synaptophysin I three-dimensional reconstruction and models of 5-fold and 7-fold imposed symmetry**

(A) Chromatogram from gel filtration purification of synaptophysin I complex. Blue curve shows calibration standards for the purification column run under synaptophysin I isolation conditions. Arrows point to peaks representing 670 kDa and 160 kDa. Red curve shows gel filtration of solubilized synaptophysin I complex isolated from bovine brain tissue. Arrow points to the peak representing the 240 kDa synaptophysin I complex as verified by SDS-PAGE and estern blot analysis. (B) SDS-PAGE analysis of (L–R) purified synaptic vesicles, final purified synaptophysin I complex, and western blot analysis of the purified complex. Arrows show marked molecular weights. (C) Fourier shell correlation curve showing the calculated resolution of the reconstruction to be approximately 20 Å based on the FSC = 0.5 criterion. (D) Reconstruction of the same single particle data as Fig. 2 with 5-fold symmetry imposed. Density is contoured to 0.5 σ.

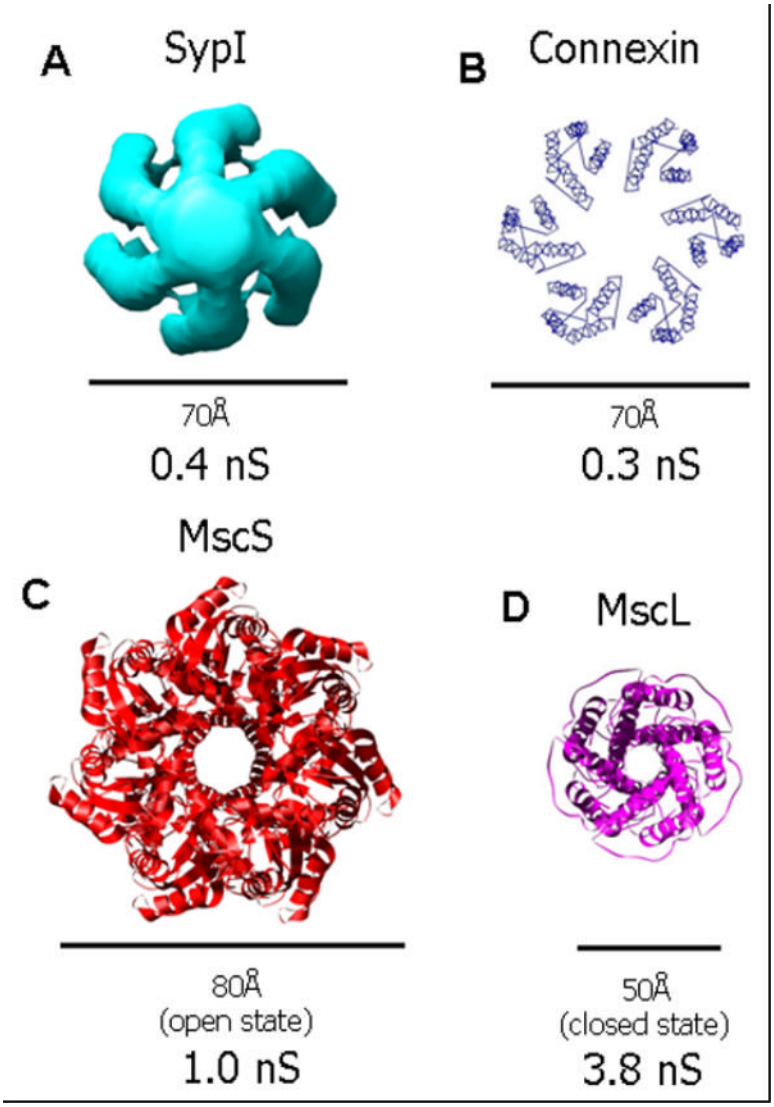


**Figure 4. Comparison of the synaptophysin I complex with other known channel structures**

(A) The synaptophysin I complex shows a similar structure and conductance to both connexin and mechanosensitive channels. Synaptophysin I has an outer diameter of 70 Å and a conductance of 0.4 nS. (B) Connexin (PDB-ID 1TXH) has an outer diameter of 70 Å and a conductance of 0.3 nS. (C) The small mechanosensitive channel MscS (PDB-ID 2OAU) has an outer diameter of 80 Å and a conductance of 1.0 nS. (D) The large mechanosensitive channel MscL (PDB-ID 2OAR) has an outer diameter of 50 Å and a conductance of 3.8 nS.

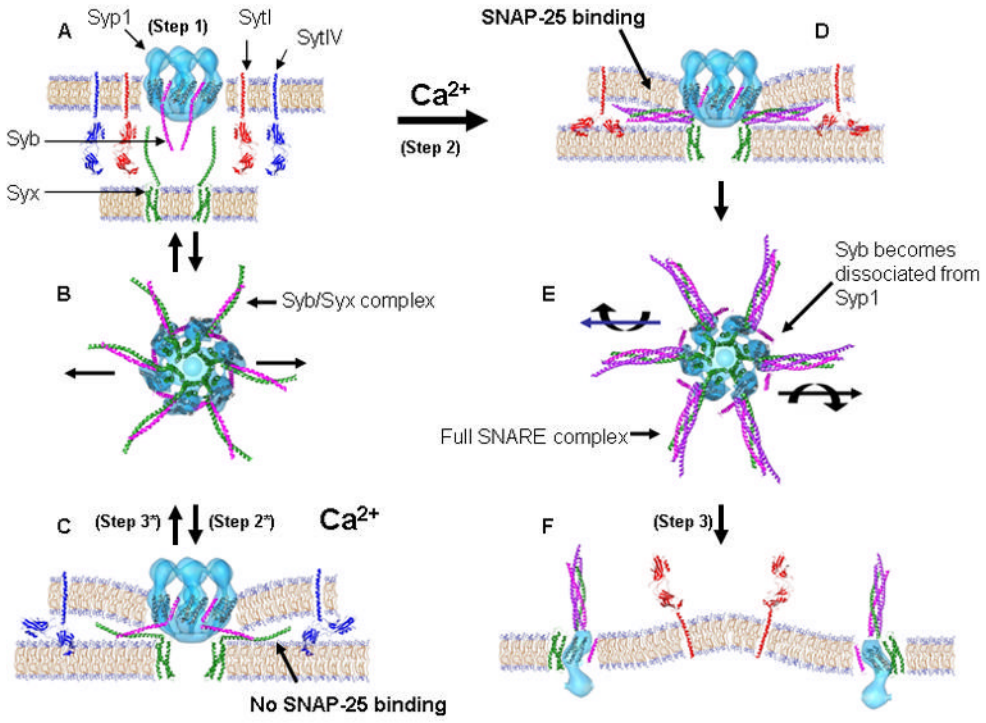


**Figure 5. Model for Synaptophysin I (Syp1) complex involvement in vesicle fusion**

Vesicles containing unassembled SNARE complexes approach the active zone of the pre-synaptic matrix. (A) Vesicles become "docked" through of t/v-SNARE interaction (step 1). Vesicle then proceed down one of two pathways: Full-fusion (FF) or Kiss-and-Run (KNR). Along the FF pathway SytI is the principal calcium sensor. Upon calcium influx, SytI binds to the SNARE complex and both C2 domains of SytI bind calcium and form a tight electrostatic interaction with the pre-synaptic membrane (E & F) which pulls the vesicle into pre-synaptic membrane. The SypI complex then binds with Syx on the plasma membrane and forms a fusion pore (step 2). The strong interaction of SytI with the pre-synaptic membrane and the tight formation of the SNARE complex disassociates Syb from Syp1 thus weaking the Syp1 complex and allowing the vesicle to fully fuse and dissociate the Syp1 hexamer (step 3). E shows a top view of the interaction of the SNARE complex and the dislodging of Syb from the Syp1 complex. In the KNR pathway SytIV is the principal calcium sensor and a weak interaction between SytIV and Syb occurs excluding SytI from interacting with Syb (B & C). Upon calcium influx only the C2B domain of SytIV binds calcium. This results in a weaker electrostatic interaction between SytIV and the pre-synaptic membrane (step 2*). The weak interaction of SytIV with the pre-synaptic membrane and the exclusion of Syb from forming a complete SNARE complex allows Syb to remain bound to the Syp1 complex and inhibits the vesicle from fully fusing (step 3*). B shows a top view of the interaction of Syb with Syx and how Syb remains bound to the Syp1 complex during transient fusion.